Open Peer Review on Qeios

Theory of the Leaky Intestine: Gender Differences in Intestinal Parasitic Infections, Cytoskeletal Wall Dysfunctions, and Hypertension

Philip Njemanze[1], Anthonia Chioma Amadi[1], Joy E. Onuchukwu[1], Chinwendu C. Darlington[1], Nneoma E. Ukeje[1], Clinton O. Mezu[1], Clara C. Ofoegbu[1], Chidera Okuh[1], Chidimma O. Ukaegbu[1], Linda O. Uzoma[1], Marvis Amuchie[1], Faustina N. Ojilere[1], Lilian C. Mbara[1], Esther C. Nneke[1]

1 Chidicon Medical Center

Funding: No specific funding was received for this work.

Potential competing interests: No potential competing interests to declare.

Abstract

Background: Intestinal parasitic infections (IPIs) impact approximately 3.5 billion individuals globally. Protozoan IPIs may influence the intestinal microbiome. This research investigates IPI effects on intestinal wall thickness and their potential links to gender-specific hypertension. It also explores the impact of alterations in intestinal wall permeability on sodium and blood glucose levels. **Methods:** The study enrolled 108 subjects, including 83 consecutive patients with confirmed symptomatic IPIs (48 males, 35 females) and 25 healthy controls (9 males, 16 females). B-mode ultrasound grayscale images of the duodenum and colon were taken with and without water contrast. **Results:** Patients with parasites exhibited a higher BMI (mean = 28.98 ± 7.43) compared to controls (mean = 24.68 ± 7.2), $F(1, 96) = 5.78$, $p < 0.05$. IPI patients showed a tendency towards increased duodenal wall thickness (DUOTHICK = 0.88 ± 0.73 cm) versus controls (0.6 ± 0.1 cm), $p = 0.056$. Additionally, IPI patients had significantly greater thickness in the ascending colon (ASCTHICK = 1.1 ± 0.3 cm) and descending colon (DSCTHICK = 1.2 ± 0.4 cm) compared to controls (ASCTHICK = 0.6 ± 0.2 cm, DSCTHICK = 0.6 ± 0.1 cm), $p < 0.05$. Men over 50 years exhibited greater DSCTHICK (1.25 ± 0.434 cm) than postmenopausal women (0.986 ± 0.389 cm), $p < 0.05$. DSCTHICK significantly predicted diastolic blood pressure ($\beta = -0.295$, $p < 0.05$) and blood sodium level ($\beta = -0.300$, $p < 0.05$). DUOTHICK in diabetic IPI patients exceeded that in nondiabetic patients. Effective antiparasitic and antidiabetic treatments induced changes in the echoanatomy of the intestinal wall, suggesting the sealing of 'the leak'. **Conclusions:** IPIs disrupted the intestinal cytoskeleton, leading to "leaky gut syndrome" development.

Philip Chidi Njemanze*, **Anthonia Chioma Amadi**, **Joy E. Onuchukwu**, **Chinwendu C. Darlington**, **Nneoma E. Ukeje**, **Clinton O. Mezu**, **Clara C. Ofoegbu**, **Chidera Okuh**, **Chidimma O. Ukaegbu**, **Linda O. Uzoma**, **Marvis Amuchie**, **Faustina N. Ojilere**, **Lilian C. Mbara**, and **Esther C. Nneke**

Chidicon Medical Center, Institute of Non-Invasive Imaging for Parasitology, International Institutes of Advanced Research and Training, Owerri 460242, Imo State, Nigeria.

*Correspondence: philip.njemanze@chidicon.com

Keywords: microbiota; parasites; ultrasound; helminth; protozoan.

1. Introduction

Globally, approximately 3.5 billion people are affected by intestinal parasitic infections (IPIs)[1]. Approximately 450 million people develop severe morbidity, and over 200 million die from IPIs, with the majority of these deaths occurring among children. According to the World Health Organization (WHO), there were 800-1000 million cases of *Ascaris lumbricoides*, 700-900 million cases of hookworm infections, 500 million cases of *Trichuris trichuria*, 200 million cases of *Giardia lamblia*, and 500 million cases of *Entamoeba histolytica*/*dispar* worldwide [2][3][4][5][6][7][8][9]. It has been demonstrated that the intestinal microbiome is influenced by IPIs, especially those caused by protozoan species [8]. It was observed that individuals infected with *E. histolytica*/*dispar* and *G. lamblia* showed a decrease in the *Collinsella* genus [8]. In Nigeria, the spatial distribution of helminthic infections such as *Ascaris lumbricoides*, hookworm, *Trichuris trichiura*, *S. stercoralis*, *Taenia* sp. *S. mansoni*, *Enterobius vermicularis*, and *Hymenolepis nana* across the six geopolitical zones has been identified [10]. The prevalence of intestinal helminths in Nigeria has not declined since the 1970s *Ascaris lumbricoides* was the most prevalent helminth in southwestern Nigeria (21%) and southern Nigeria (13%). Hookworm was the most prevalent helminthic infection in southeastern Nigeria, accounting for 19% of cases. On the other hand, there were multiple infections in northern Nigeria, with 25% in the northcentral zone and 19% in both the northeast and northwest zones, respectively. There was a high prevalence of *Taenia* species and *Schistosoma mansoni* infections in the northeast and northwest zones of Nigeria, reported at rates of 8% and 6%, respectively [10]. In Owerri West Local Government Area in Imo State, southeastern Nigeria, the prevalence of soil-transmitted helminths among primary school pupils was 35.43% [11]. In Owerri Municipal LGA, the overall prevalence of helminths among children in daycare centers was 58% [12].

The role of the human intestinal microbiome in health and disease has gained significant attention in recent years. Some investigators have suggested that the intestinal microbiome may vary between males and females. The divergence in the intestinal microbiome observed between men and women may be related to the gender differences observed in the prevalence of hypertension, metabolic disorders, and intestinal inflammatory diseases. Some researchers have suggested that gender differences may be influenced by the level of obesity [13]. There are clear gender differences in cardiovascular disease. Women experience cardiovascular events at an older age, and on average, they have less atherosclerotic plaque than men, regardless of age [13]. Furthermore, men and women are known to have gender-specific differences in their immune systems and intestinal microbiome composition [14].

Several cross-sectional studies in humans have shown an association between the intestinal microbiome and hypertension [15][16][17][18][19][20][21][22][23][24]. Globally, it is estimated that there are 1.28 billion adults aged 30-79 with hypertension. Over 75% of patients with hypertension live in low- and middle-income countries. In Nigeria, the prevalence

of hypertension has increased from 8.2% in 1990 to 32.5% in 2020 [25]. Some studies have even suggested a prevalence of hypertension as high as 38% [26]. There is a gender difference in the prevalence of hypertension. The prevalence of hypertension was higher among men up to the age of 50. However, beyond that age, females experienced higher rates in every age group [27]. In Nigeria, most studies have shown that the prevalence of hypertension is higher in men than in women [28].

It is interesting to explore whether there is a causal link between the high prevalence rates of IPIs and hypertension in Nigerians. If so, could effectively treating IPIs in early childhood and adulthood reduce the occurrence of hypertension in elderly Nigerians?

The IPIs cause dysfunction in the intestinal cytoskeleton, which in turn presumably promotes dysbiosis of the intestinal microbiome [29]. The causal relationship between dysbiosis and hypertension remains inconclusive. The specific mechanism by which the intestinal microbiome affects the progression of hypertension remains unclear. It is therefore interesting to investigate the interaction between the intestinal cytoskeleton and hypertension. It has been postulated that there are key mechanisms regulating the effects of the intestinal microbiome on hypertension [30]. It has been proposed that intestinal dysbiosis leads to disruptions in the nervous system, renal function, the production of short-chain fatty acids (SCFAs) in the intestines, the immune system, and an increase in the production of lipopolysaccharide (LPS) and intestinal permeability. These factors can aggravate the progression of hypertension [30].

Recently, we used ultrasound duodenography and colonography to illustrate that IPI-induced thickening of the intestinal wall, along with rearrangement of the cytoskeleton, resulted in dysfunction of the glucose transporter system. This dysfunction ultimately resulted in the development of type 2 diabetes mellitus (T2DM) [29]. The inflammatory processes associated with IPIs lead to an increase in the thickness of the intestinal wall. This increase can be measured as a surrogate marker for intestinal cytoskeletal dysfunction using high-frequency ultrasound duodenography and colonography [29][31][32][33].

The purpose of this study is to investigate gender differences in the interaction between intestinal cytoskeletal dysfunction and hypertension. We postulate a theory based on our earlier hypothesis that, due to the effects of IPIs causing intestinal wall cytoskeletal dysfunction, the intestinal wall becomes ‘leaky’ to the microbiome, sugar, salts, and other metabolites and causes imbalance of the sympathetic nervous system [34], which in turn exacerbates the risk of hypertension and metabolic and intestinal inflammatory diseases. Moreover, increased sympathetic tone has been linked to elevated inflammation both systemically and in the intestine [35], which could contribute to vascular gastrointestinal leakage[36]. “We are going to investigate the impact of effective anti-parasitic and anti-diabetic treatments on the echo-anatomy of the intestinal wall”. Furthermore, we propose innovative ways of ‘sealing the leak’ on the intestinal wall [37].

2. Methods

In this study, 108 participants were recruited, including 83 consecutive patients (48 males and 36 females) with symptomatic and laboratory-confirmed IPIs, as well as 25 healthy controls (9 males and 16 females). A standardized

questionnaire was used to collect clinical symptoms and disease history, including information about the onset and duration of the illness. Qualitative and quantitative aspects of the illness, including the intensity and periodicity of abdominal pain, were recorded. The body mass index (BMI), fasting blood glucose (FBG), systolic and diastolic blood pressure, blood sodium, and potassium levels were also monitored. The patient population was classified into three groups based on the onset and duration of illness at presentation: (1) acute—within 1 month or less, (2) subacute—within the past 12 months or less, and (3) chronic—after 12 months. Exposure to contaminated food or water was recorded for each participant. Patients with parasitic infections who presented with rectal bleeding underwent colonoscopy to rule out the possibility of colorectal cancer. Patients with a history of alcoholism, ulcerative colitis, major gastrointestinal diseases such as polyposis, collagen vascular diseases, pancreatic diseases, liver diseases, Crohn's disease, tropical sprue, colon cancer, and diverticulitis were excluded from the study. The institutional human research ethics review board approved the protocol.

2.1. *Laboratory Stool Ova and Parasite Tests*

The laboratory stool ova and parasite test involved the microscopic detection of IPIs in fecal smears from three individual specimens or duodenal aspirates. Wet preparations of stool samples were examined by two parasitologists, and any discrepancies were resolved by a third parasitologist who was not involved in the initial evaluation [29][31][32][33]. The quantitative evaluation of IPIs in stool samples was based on the count per high-power field (HPF) of view. The quantitative estimation in stool samples, based on the count per hpf of view, was rated as follows: (1) controls with 0-1 IPI per hpf; (2) mild with 2-4 IPIs per hpf; (3) moderate with 5-10 IPIs per hpf; and (4) severe with (more than 10) IPIs per hpf. In follow-up studies, a negative stool test or a reduced count of intestinal parasites per hpf was used as an indicator of recovery. Patients underwent a comprehensive panel of standard laboratory blood tests, including measurements of a complete blood count, liver and kidney function, lipid profile, and glucose levels [38].

2.2. *High-Frequency Ultrasound Duodenography and Colonography*

The protocol for high-frequency ultrasound duodenography and colonography was described in detail elsewhere [29][31][33]. Traditional abdominal ultrasound examinations were performed using B-mode and color flow Doppler ultrasonography. A low-frequency transducer (2.5 MHz) from a phased array transducer (S4 probe) was utilized with a duplex color flow Doppler ultrasound system (Agilent HP/Philips SONOS 5500, Philips Medical Systems, Cambridge, MA, USA) [29]. The abdominal ultrasound scan examined the internal organs, including the liver, gall bladder, spleen, pancreas, duodenum, colon, and kidneys, in all subjects [29][31][33]. Briefly, the high-frequency ultrasound duodenography examined the walls and folds of the duodenum using a 7.5 MHz probe, starting in the right hypochondriac (1) and epigastric (2) regions (see Figure 1A). Using the 7.5 MHz probe, the ultrasound colonography evaluated the walls and haustra of the ascending colon, starting from McBurney's point, which is located at one-third of the distance laterally on a line drawn from the umbilicus to the right anterior superior iliac spine. This technique has been described in detail elsewhere [29][31][32][33]. The examination proceeds upward to the right lumbar (4), right hypochondriac (1), and then turns clockwise to the epigastric (2), left hypochondriac (3), left lumbar (6), and left iliac (9) regions. The ultrasound examination

utilized color flow Doppler to assess the localization of lesions in relation to vessels [29]. The ultrasound examination was used to detect the presence of comorbid conditions [29].

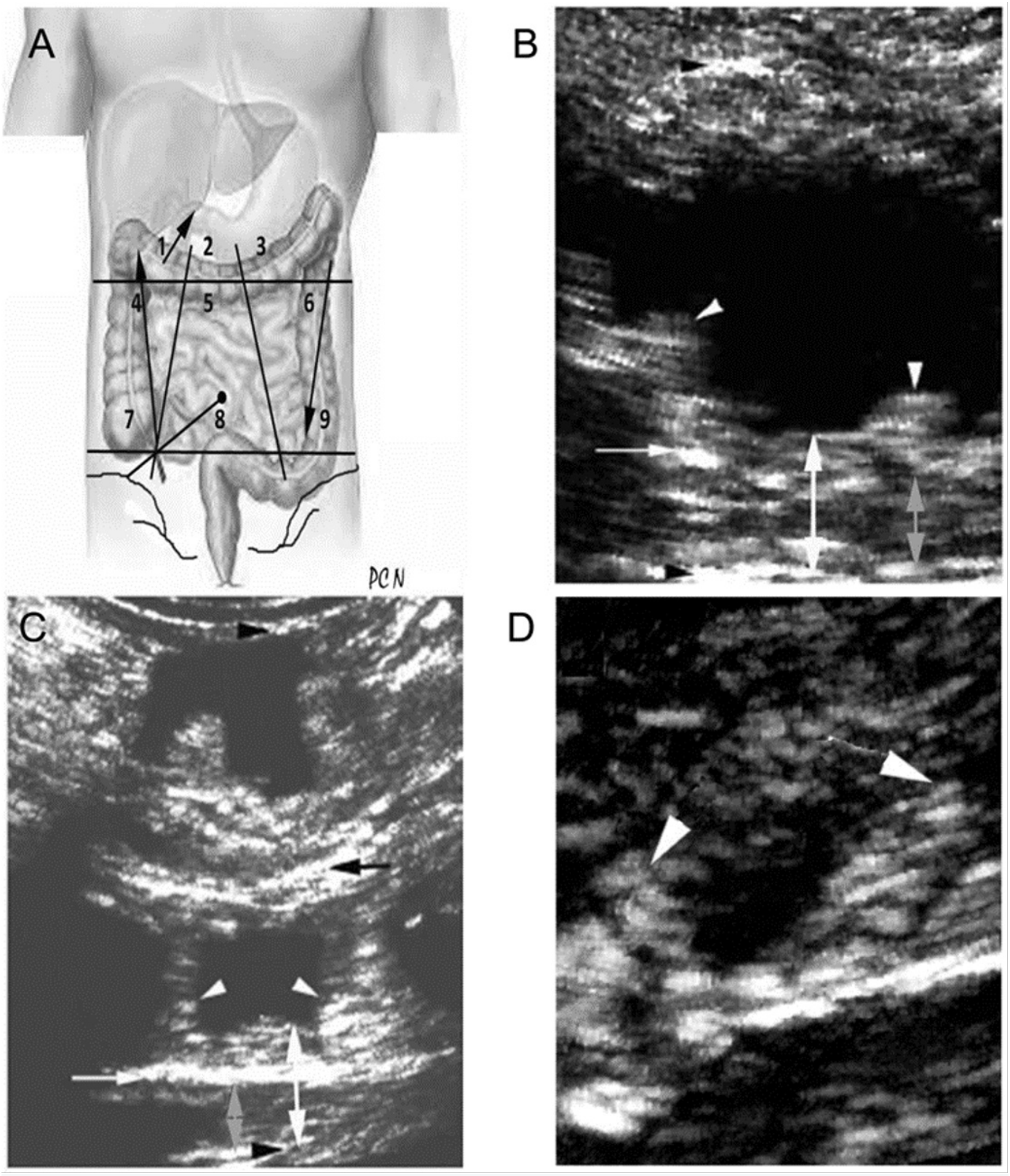

Figure 1. (**A**–**D**). (**A**). Locations on the abdominal wall for placing a transducer for examining the intestine. The examination proceeds upward to the right lumbar visualizing the cecum (7) upwards the ascending colon (4), right hypochondriac (1), and then turns clockwise to the epigastric (2), left

hypochondriac (3), visualizing the transverse colon (5), downwards to the left lumbar (6), along the descending colon, to the left iliac (9) regions to the sigmoid colon (8) below the umbilicus. (**B**). Duodenometrics illustrating measurement endpoints during duodenal examination using water contrast imaging. (**C**). Colometrics displaying measurement endpoints in the ascending and (**D**) descending colons with water contrast, revealing pyramidal-shaped haustra (indicated by white arrowheads). Details of duodenometric and colometric measurements are given in the text.

The results of the stool analysis were preceded by high-frequency ultrasound duodenography and colonography examinations. All ultrasound scans were performed with and without water contrast after overnight fasting (for at least 16 h) using the scanning procedure described in detail elsewhere [31][33]. The water contrast imaging was performed by instructing the subjects to consume at least 1 L of water prior to the examination [31][33]. The subject was placed in the supine horizontal, left posterior oblique, and left lateral decubitus positions using the intercostal and subcostal approaches [31][33].

All measurements and grading of echogenicity were performed by a single trained sonographer using the built-in software. Measurements were taken between peristaltic waves. The measurements of the duodenum (duodenometrics), ascending colon, and descending colon (colometrics) were performed using water contrast imaging [31][33]. The measurement endpoints used to characterize dysfunction in the intestinal cytoskeleton were the thicknesses of the intestinal walls [31][33]. The measurement of duodenal wall thickness (DUOTHICK) was performed using duodenal metrology techniques. This involved measuring the distance between two mucosal folds of Kerckring [31][33], starting from the surface of the moderately echogenic mucosa, passing through the hyperechoic submucosa and hypoechoic muscularis, and ending at the hyperechoic serosa layer. Similarly, the colometric measurement of the ascending colon wall thickness (ASCTHICK) and descending colon wall thickness (DSCTHICK) was taken between two haustra across all three layers of the wall [31][33].

The lesion in each subject was characterized by several factors, including its location, wall thickness, echogenicity of the intestinal wall tissue, presence or absence of flattening or loss of duodenal folds and/or colonic haustration, presence or absence of hyperechoic floating foci (HFF) demonstrating chaotic and/or bulk motility, presence or absence of perilesional tissue echogenicity, and type of colonic peristalsis [29][31][33]. The IPI lesions were due to the presence of protozoa and/or helminths [29]. The helminthic parasites were visible macroscopic organisms that appeared as hyperechoic curvilinear foci (HCF) and exhibited serpentine motility [31]. The protozoan parasites were microscopic organisms that could be observed as lesions on echogenic floaters. The flagellates, such as *Giardia lamblia*) or ciliated parasites, use floaters to exhibit chaotic motility. This is characterized by rapid flotation movements in all directions, as observed sonographically by HFF, in between peristaltic waves. On the other hand, floaters used for amebic lesions demonstrated bulk motility. Bulk motility is defined as the sonographically observed slow floating movements of HFF in mainly one direction between peristaltic waves.

2.3. *Antiparasitic Treatment*

The treatment regimen for protozoal infections consists of either intravenous infusion of metronidazole (500 mg in 100 mL) or oral administration of one tablet (500 mg) or two tablets (250 mg) three times a day for 10 days [29]. The treatment

regimen for helminthiasis consists of oral administration of albendazole (400 mg) twice a day for 3 days [29]. In most patients with IPIs, the treatment regimens for both protozoa and helminthes were combined.

2.4. *Blood Pressure Classification*

The blood pressure classification followed the guidelines set forth in the Seventh Report of the Joint National Committee on Prevention, Detection, Evaluation, and Treatment of High Blood Pressure [39].

2.5. *Statistical Analysis*

Statistical analysis was conducted using descriptive statistics, t-test, regression, and analysis of variance (ANOVA) for group comparison with the IBM SPSS Statistics software package for Windows, version 28.0.1.1. (15) (IBM Corp., Armonk, NY, USA). Mean values were presented as mean ± standard deviation (SD). The statistical analysis excluded patients with one or more missing values within a group, and mean substitution was not employed. The level of statistical significance was established at $p < 0.05$. However, values exceeding this threshold were considered non-significant ($p = NS$).

3. Results

Patients with IPIs exhibited a range of symptoms, including abdominal pain, particularly in the right upper quadrant, flatulence, nausea, vomiting, borborygmi, perceived weight loss, and occasional episodes of constipation or diarrhea. Ten patients also experienced occasional severe hematochezia. Stool analysis of patients with IPIs revealed the presence of ova and parasites from various micro-organisms, including *Entamoeba histolytica*, *Entamoeba coli*, *Giardia lamblia*, *Ascaris lumbricoides*, hookworm, *Trichuris trichiura*, and *Taenia* species. In contrast, healthy individuals did not manifest any of these symptoms.

3.1. *Sonographic Findings and Duodenometrics in a Normal Duodenum*

High-frequency ultrasound revealed the duodenal wall as alternating bands of moderately echogenic mucosa with a hyperechoic core submucosa. These bands form folds known as Kerckring's folds, arranged in a circular pattern. The duodenal wall comprises of a middle hypoechoic muscularis layer and an outer hyperechoic serosa layer [31]. The measurement parameters for the duodenal layers are termed duodenometrics. This measurement indicates the wall thickness endpoints of the duodenum (with water contrast) (Figure 1B; indicated by double white arrow ends). It is measured between two Kerckring's mucosal folds [31] (Figure 1B; indicated by white arrowheads), starting from the surface of the moderately echogenic mucosa, traversing the hyperechoic submucosa (Figure 1B; indicated by a white arrow), the hypoechoic muscularis (Figure 1B; indicated by double gray arrowheads), and concluding at the hyperechoic serosa layer (Figure 1B; indicated by the bottom black arrowhead). Duodenometric measurements in patients and control subjects are given in Table 1.

Table 1. The study assessedparameters and provideddescriptive statisticsfor patients with IPIs and control subjects .

Parameters		Descriptive Statistics						
	Gender	N	Mean ± SD	Gender Difference p	N	Mean ± SD	Gender Difference p	Patients vs. Controls p
	Patients with IPIs				Control Subjects			
Age	Female	35	50.6 ± 16.2	NS	16	53.2 ± 15.8	0.01	NS
	Male	48	49.7 ± 16.7		9	37.8 ± 10.5		0.05
	Total	83	50.1 ± 16.4		25	47.4 ± 15.7		NS
BMI	Female	32	30.3 ± 8.9	NS	14	26.2 ± 5.2	NS	NS
	Male	44	28.1 ± 6.1		8	22.1 ± 9.8		0.05
	Total	76	28.9 ± 7.4		22	24.68 ± 7.2		0.05
FBG (mg/dL)	Female	28	112.1 ± 43.9	NS	14	136.2 ± 75.1	NS	NS
	Male	32	118 ± 47.7		7	98.7 ± 28.7		NS
	Total	60	115.3 ± 45.6		21	123.7 ± 65.1		NS
Systolic Blood Pressure (mmHg)	Female	35	141.3 ± 24.7	NS	16	143.9 ± 22.3	NS	NS
	Male	48	138.8 ± 21.6		9	145.3 ± 33.4		NS
	Total	83	139.8 ± 22.8		25	144.4 ± 26.1		NS
Diastolic Blood Pressure (mmHg)	Female	35	85.8 ± 12.7	NS	16	89.1 ± 12.3	NS	NS
	Male	48	85.9 ± 17.5		9	86.7 ± 11.4		NS
	Total	83	85.8 ± 15.6		25	88.2 ± 11.8		NS
Sodium (mEq/L)	Female	35	154.6 ± 34.8	NS	15	166.9 ± 33.8	NS	NS
	Male	47	160 ± 38.5		9	166 ± 40		NS
	Total	82	157.7 ± 36.8		24	166.6 ± 35.6		NS
Potassium (mEq/L)	Female	34	5.3 ± 7.2	NS	15	4.4 ± 1.8	NS	NS
	Male	47	4.4 ± 1.1		9	3.5 ± 0.4		0.05
	Total	81	4.8 ± 4.7		24	4.1 ± 1.5		NS
Duodenal Wall Thickness (cm)	Female	33	0.75 ± 0.2	NS	16	0.6 ± 0.1	NS	0.01
	Male	48	0.97 ± 0.9		9	0.6 ± 0.1		NS
	Total	81	0.88 ± 0.7		25	0.6 ± 0.1		0.05
Ascending Colon Wall Thickness	Female	34	1.1 ± 0.3	NS	16	0.6 ± 0.2	NS	0.0001
	Male	48	1.1 ± 0.3		9	0.6 ± 0.2		0.0001
	Total	82	1.1 ± 0.3		25	0.6 ± 0.2		0.0001
Descending Colon Wall Thickness	Female	32	1.2 ± 0.3	NS	14	0.7 ± 0.2	NS	0.0001
	Male	44	1.2 ± 0.4		9	0.6 ± 0.2		0.0001
	Total	76	1.2 ± 0.4		23	0.6 ± 0.1		0.0001

3.2. *Sonographic Findings and Colometrics in a Normal Colon*

The colonography image in Figure 1C displays the colonic wall, which comprises alternating hypoechoic and hyperechoic bands corresponding to the histological layers. The colonic wall exhibits a moderately echogenic mucosa, a hyperechoic core submucosa, a hypoechoic muscularis layer, and an outer hyperechoic serosa [31][32]. In the mid-section, the outer layer of the colon's longitudinal muscle displays a relatively hyperechoic structure known as the *tenia coli librae* (Figure 1C; black arrow). The pyramid-shaped haustra have an isoechoic appearance with the mucosa (Figure 1C; white arrowheads). The colon's wall thickness (Figure 1C; with water contrast, indicated by double white arrowheads) is measured between two haustra (Figure 1C; indicated by white arrowheads). This measurement originated from the surface of the moderately echogenic mucosa (Figure 1C; top arrow of the double white arrows), passing through the hyperechoic submucosa (Figure 1C; white arrow), and hypoechoic muscularis (Figure 1C, indicated by double gray arrow ends) layers, and reaching the hyperechoic serosa layer (Figure 1C; indicated by the bottom black arrowhead, representing the haustra with a pyramidal shape). Figure 1D (white arrowheads) displays a pyramid-shaped haustra in the descending colon, featuring a regular contour, uniform appearance, and equidistant spacing. The colometric measurements in patients and control subjects are given in Table 1.

3.3. *General Effects*

The parameters and descriptive statistics measured in patients with IPIs and the control subjects in the study are presented in Table 1. A one-way ANOVA was conducted to investigate the impact of parasites on various dependent variables, such as age, BMI, FBG, SBP, DBP, blood sodium levels (Na+), and potassium (K+) levels. The results revealed that there was no significant difference in age between patients with parasites (mean age = 50.1 ± 16.4 years) and the control group (mean age = 47.4 ± 15.7 years), $p = NS$. However, male patients with parasites (mean age = 49.7 ± 16.7 years) were older compared to the control group (mean age = 37.8 ± 10.5 years), $p < 0.05$. Patients with parasites had a significantly higher BMI (mean = 28.98 ± 7.43) compared to the control group (mean = 24.68 ± 7.2), $F(1, 96) = 5.78$, $p < 0.05$. However, there was no gender-related difference in BMI, FBG, SBP, DBP, Na+, and K+ between men and women.

To investigate the impact of IPIs on intestinal wall thickness, a one-way ANOVA was conducted. The purpose was to compare the effects of chronic parasitic infection on patients and control subjects. The dependent variables analyzed were DUOTHICK, ASCTHICK, and DSCTHICK. The results indicated that patients with parasites exhibited a tendency towards a statistically significant difference in DUOTHICK (mean = 0.88 ± 0.73 cm) compared to controls (mean = 0.6 ± 0.1 cm), $F(1, 104) = 3.73$, $p = 0.056$. There was a significant difference in ASCTHICK between patients with chronic parasites (mean = 1.1 ± 0.3 cm) and the control group (mean = 0.6 ± 0.2 cm), $F(1, 105) = 59.4$, $p < 0.001$. Similarly, there was a significant difference in DSCTHICK between patients with chronic parasites (mean = 1.2 ± 0.4 cm) and the control group (mean = 0.6 ± 0.1 cm), $F(1, 97) = 49.97$, $p < 0.001$.

To investigate the impact of gender in patients with chronic parasitic lesions over 50 years old, a one-way ANOVA was conducted. The results demonstrated that in men, the thickness of the descending colon (DSCTHICK = 1.25 ± 0.434 cm) was greater than that in postmenopausal women (AGE > 50 years) (DSCTHICK = 0.986 ± 0.389 cm), $F(1, 49) = 5.5$, $p <$

0.05. However, no significant gender-related difference was observed in other parts of the intestine (DUOTHICK and ASCTHICK). Additionally, for patients younger than 50 years, there was no significant difference in the thickness of the descending colon wall between men (DSCTHICK = 0.965 ± 0.439 cm) and premenopausal women (AGE < 50 years) (DSCTHICK = 1.068 ± 0.342 cm), $p = NS$.

To investigate the relationship between the thickness of the descending colon's wall and diastolic blood pressure, a linear regression model was employed. This model quantified the relationship between the predictor variable DSCTHICK and the response variable DBP in patients with chronic parasitic lesions. Simple linear regression was used to determine if DSCTHICK significantly predicted DBP. The fitted regression model was DBP = 100.822 – 12.367 × (DSCTHICK). The overall regression was statistically significant (adjusted $R^2 = 0.075$, $F(1, 74) = 7.055$, $p < 0.05$). The result showed that the thickness of the intestinal wall in the descending colon significantly predicted diastolic blood pressure ($\beta = –0.295$, $p < 0.05$). In other words, DSCTHICK varied inversely with DBP. However, the thickness of the intestinal wall in the descending colon did not predict systolic blood pressure ($p = NS$).

3.4. *Sodium Absorption through the 'Leaky Intestine'*

To examine the relationship between the thickness of the intestinal wall in the descending colon of patients with parasitic lesions and their blood sodium levels, a linear regression model was utilized. The blood sodium level depends on the osmotic gradient on either side of the intestinal brush-border membrane (BBM) [40]. A simple linear regression was performed to determine if DSCTHICK significantly predicted the Na+ level in the blood. The fitted regression model was Na+ = 193.367 – 29.77 × (DSCTHICK). The overall regression was statistically significant (adjusted $R^2 = 0.077$, $F(1, 73) = 7.197$, $p < 0.05$). The findings indicated that the thickening of the intestinal wall in the descending colon significantly predicted the blood sodium level ($\beta = –0.300$, $p < 0.05$). In other words, DSCTHICK varied inversely with the blood Na^+ level. It is plausible that the thickening of the descending colon wall, caused by parasite-induced cytoskeletal wall dysfunction, resulted in a thicker and less permeable intestinal wall for sodium salts. This could have contributed to the reduction in diastolic blood pressure levels, but not systolic blood pressure. Moreover, the relationship between the thickness of the intestinal walls in the duodenum (DUO), ascending colon (ASC), and descending colon (DSC) was specifically investigated in males with parasitic infections and blood sodium levels. A multiple linear regression model was employed to determine if the predictors DUOTHICK, ASCTHICK, and DSCTHICK significantly predicted the response of Na+. The overall regression was statistically significant (adjusted $R^2 = 0.179$, $F(3, 39) = 4.047$, $p < 0.05$). The predictor DUOTHICK was found to significantly predict the response of Na+ levels ($\beta = –0.295$, $p < 0.05$). Similarly, the predictor DSCTHICK significantly predicted the Na+ level response ($\beta = –0.387$, $p < 0.05$). However, the predictor ASCTHICK did not significantly predict the Na+ blood level response ($\beta = –0.578$, $p = NS$).

3.5. *Bleeding through the 'Leaky Intestine'*

The 'leaky intestine' is susceptible to bleeding. Ten patients with IPIs had a history of repeated severe hematochezia, abdominal pain, constipation, persistent flatulence, borborygmi, and lactose intolerance. We conducted tests for levels of

carcinoembryonic antigen (CEA) and performed a colonoscopy to rule out bowel cancer. A typical case finding is described below as an example. A 48-year-old male presented with hematochezia, abdominal pain, constipation, persistent flatulence, borborygmi, and lactose intolerance. The symptoms began two years ago, when he suddenly noticed hematochezia. He consumes fresh garden eggs (*Solanum aethiopicum*) and African star apple (*Chrysophyllum albidum*), which might expose him to parasites found in soil contaminated with human waste in the environment. Upon admission, the blood pressure was 142/81 mmHg, and his pulse was 73 bpm. Laboratory tests indicated a hematocrit of 42%, hemoglobin of 14.1 g/dL, a white blood cell count of 3,500/mm^3, an ESR of 11 mm/hr, a clotting time of 10 min, a platelet count of 185,000/mm^3, a prothrombin time of 26 s, hypernatremia (sodium of 166 mEq/L), chloride of 92 mEq/L, potassium of 6 mEq/L, and calcium of 10.8 mg/dL. Liver function tests showed normal levels of alanine transaminase (ALT) at 8 IU/L, aspartate transaminase (AST) at 7 IU/L, and conjugated bilirubin (CB) at 0.21 mg/dL, but elevated total bilirubin (TB) at 0.62 mg/dL. The D-dimer was normal at 0.478 mg/L of fibrinogen equivalent units (FEU). The colonoscopy did not reveal any growths (polyps) or cancer. There were no major bleeding sites or signs of inflammation. The internal hemorrhoidal complexes were engorged circumferentially, and some had shallow ulcerations. The posterior hemorrhoid bundle had grade 1 hemorrhoids that bleed but do not prolapse.

The thickness of the duodenal wall was measured pretreatment (DUOTHICK of 0.663 cm). However, after treatment, the thickness decreased (DUOTHICK of 0.32 cm). Similarly, in the ascending colon, the pretreatment wall thickness was measured (ASCTHICK of 1.02 cm), but after treatment, the thickness decreased (ASCTHICK of 0.663 cm).

Before treatment, the ultrasound image of the descending colon (Figure 2A) showed changes in echoanatomy, including increased wall thickness (DSCTHICK = 1.64 cm) (Figure 2A, marked with a double white star), decreased wall echogenicity, and rearrangement of the tri-layer wall structure. There was also haustral unfolding and occasional HFF with chaotic motility (Figure 2A, marked with a white arrowhead). However, after ten days of treatment, the post-treatment ultrasound image of the descending colon (Figure 2B) showed increased echogenicity of the walls and haustra, and the wall thickness had reduced (DSCTHICK of 0.82 cm) (Figure 2B, marked with a double white star). The follow-up post-treatment ultrasound image (Figure 1C) taken three months later showed a slight increase in wall thickness (DSCTHICK) of 0.943 cm. Nevertheless, there was a remarkable change in wall echogenicity, showing a normal tri-layer wall arrangement. The wall exhibited hyperechoic mucosa and submucosa layers, a hypoechoic muscularis layer, and a hyperechoic serosa layer.

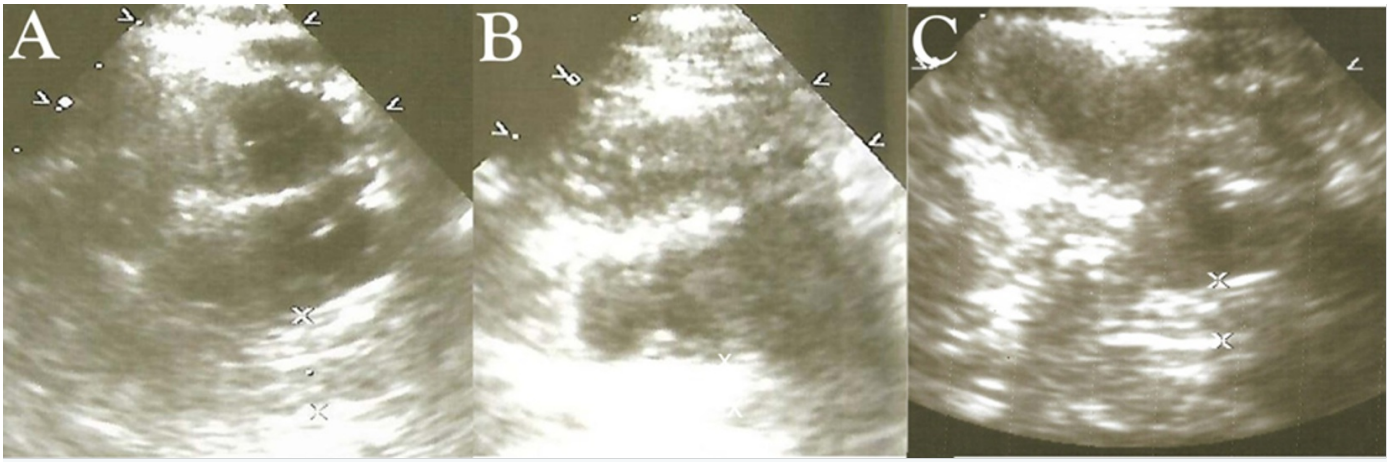

Figure 2. (**A**–**C**) display the pretreatment image (**A**), the post-treatment image taken after 10 days (**B**), and the follow-up post-treatment image captured 3 months later (**C**) with white star markers indicating wall thickness.

The pretreatment ultrasound image of the sigmoid colon (Figure 3A) revealed numerous HFF with chaotic motility (indicated by black arrowhead in Figure 3A) along with increased echogenicity and wall thickness (SIGMOID of 0.69 cm). The patient experienced persistent rectal bleeding. However, in the post-treatment image taken 3 months later (Figure 3B), there was no longer evidence of rectal bleeding or HFF. The wall thickness (measured at SIGMOID) was 0.443 cm, and the echogenicity had significantly decreased.

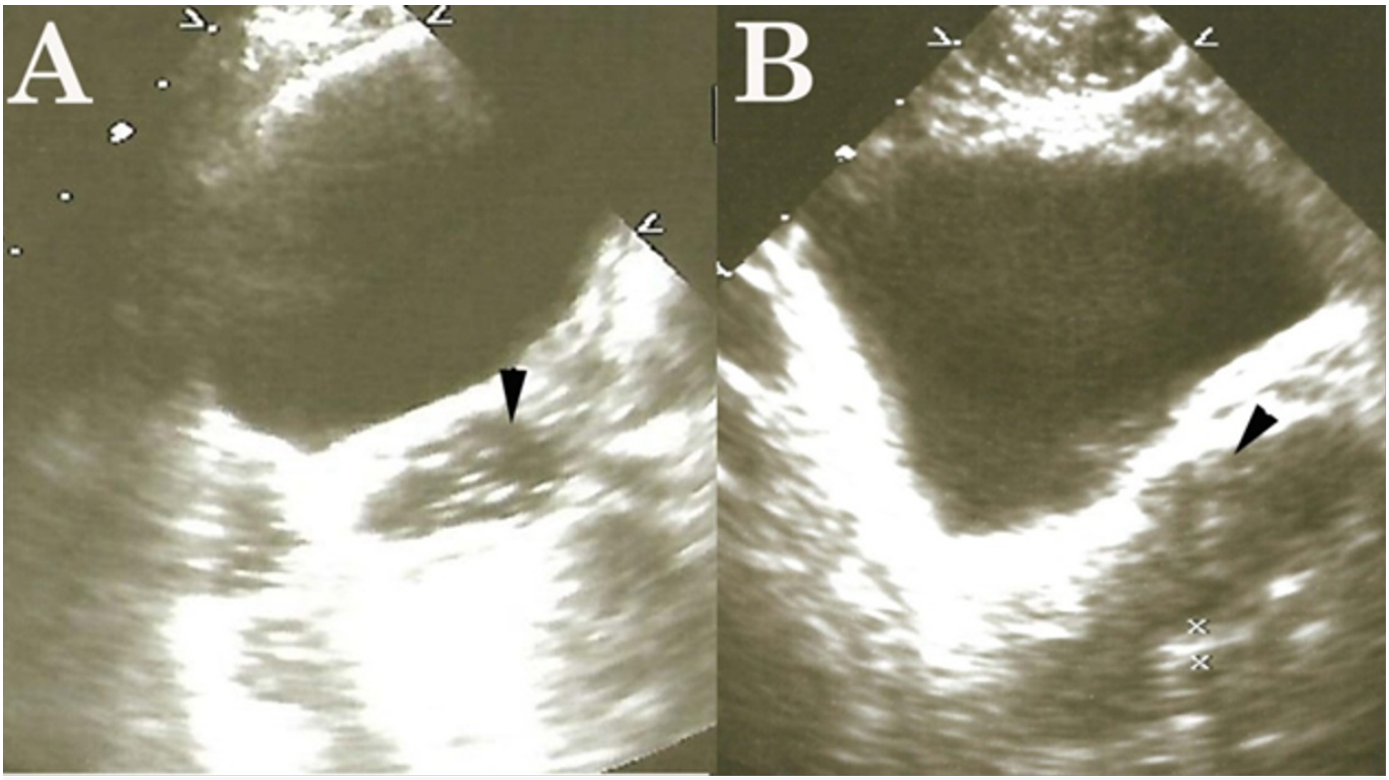

Figure 3. (**A**, **B**) displays the pretreatment image (**A**) of the sigmoid colon and rectum with abundant HFF (black arrowhead), and highly echogenic increased wall thickness. The post-treatment image (**B**) reveals a decrease in wall thickness and echogenicity, as well as the absence of HFF in the sigmoid colon (indicated by black arrowheads).

The pretreatment images (Figure 4A, B), obtained during colonoscopy, show bleeding sites (Figure 4A) in the descending colon. The mucosal and submucosal layers of the descending colon exhibit abnormally tortuous and engorged veins, a condition known as angiodysplasia. The patients were followed up for at least three months, during which significant improvements were observed in clinical presentation, as well as in ultrasound and stool test control. In cases where complaints and control tests suggested incomplete clearance of IPIs, a repeat regimen using metronidazole and albendazole was administered.

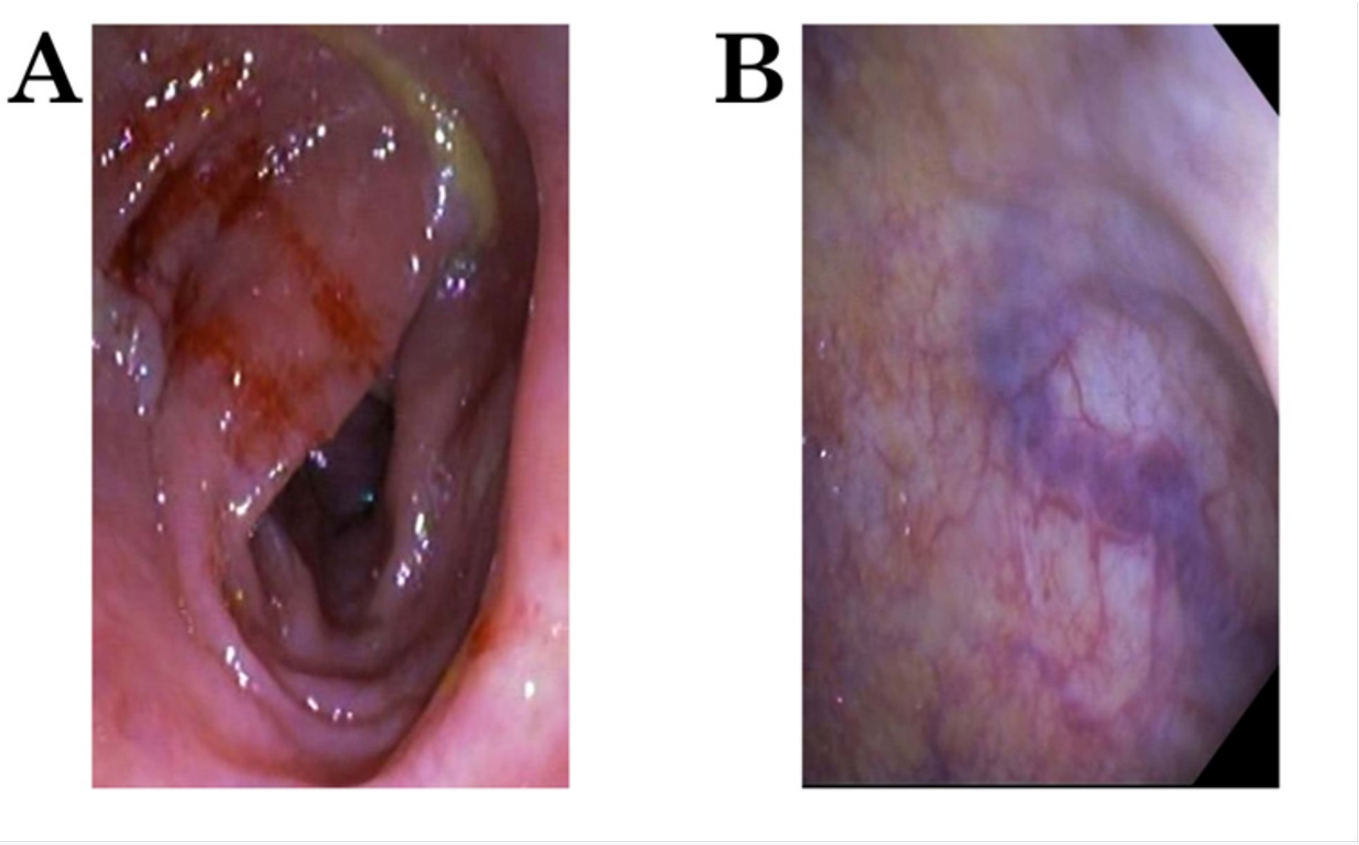

Figure 4. (**A**, **B**) shows the pretreatment images obtained during colonoscopy. The images depict bleeding sites in the descending colon (Figure 4A), and angiodysplasia [Figure 4B].

3.6. *Leaky Intestine and Sugar*

We propose that the absorption of blood glucose through a 'leaky intestine' would be abnormal. Specifically, we compared the thickness of the intestinal wall in the duodenum (DUO), ascending colon (ASC), and descending colon (DSC) in patients with IPIs. The study included a total of 81 patients, with 13 of them being diabetic and the remaining 68 being nondiabetic. The DUOTHICK (1.3 ± 1.7 cm) in diabetic patients with IPIs was greater than that in nondiabetic patients (0.8 ± 0.3 cm), $F(1, 80) = 4.3$, $p < 0.05$. However, the intestinal wall thickness of the ASCTHICK and DSCTHICK was the same for diabetic and nondiabetic patients with IPIs.

A sample case of a diabetic patient is hereby presented. A 56-year-old male presented with abdominal discomfort, constipation, persistent flatulence, borborygmi, and lactose intolerance. The symptoms began four years ago, when he

was diagnosed with IPIs and diabetes. Prior to the onset of the illness, he consumed fresh garden eggs (*Solanum aethiopicum*), which exposed him to parasites present in soil contaminated with human waste in the environment. The blood pressure was 125/81 mmHg, and the pulse was 106 bpm. Laboratory tests showed a hematocrit of 33.6%, hemoglobin of 11.2 g/dL, a white blood cell count of 3500/mm^3, an ESR of 58 mm/h, a clotting time of 8 min, a platelet count of 195,000/mm^3, prothrombin time of 38 s, hypernatremia (sodium of 264 mEq/L), chloride of 46 mEq/L, and potassium of 3.6 mEq/L. There was normal blood urea of 10 mg/dL and creatinine of 0.5 mg/dL. Liver function tests showed elevated alanine transaminase (ALT) at 34 IU/L, aspartate transaminase (AST) at 21 IU/L, conjugated bilirubin (CB) at 0.7 mg/dL, and the total bilirubin (TB) at 1.8 mg/dL. The lipid profile was within normal range, with a total cholesterol (TCHOL) of 113 mg/dL, high-density lipoprotein (HDL) of 51 mg/dL, low-density lipoprotein (LDL) of 42 mg/dL, triglycerides (TG) of 100 mg/dL and very low-density lipoprotein (VLDL) of 20 mg/dL. The pretreatment FBG was elevated at 232 mg/dL, and as well as the HbA1C at 8.7%. The initial ultrasound image (Figure 5A) showed changes in echoanatomy, including increased thickness of the duodenal wall (DUOTHICK = 1.1 cm) (Figure 5A, double white arrowheads), increased echogenicity of the wall, rearrangement of the tri-layer wall structure, loss of duodenal folds of Kerckring, and presence of HFF (Figure 5A, white arrowhead) in the duodenal lumen. The patient was treated for IPIs with intravenous metronidazole and tablets of albendazole. The T2DM was managed with Synjardy, a combination of empagliflozin (12.5 mg) and metformin hydrochloride (1000 mg), one tablet twice a day, along with diet and exercise. The mechanism of action informed the choice of the drugs, empagliflozin, and metformin hydrochloride, which belong to the class of antidiabetics: SGLT2 inhibitors and biguanides, respectively [38]. The SGLT2 transporter is highly expressed in the kidney. The post-treatment (HbA1C = 7.2%) ultrasound image of the duodenum (Figure 5B) taken three months later shows remarkable transformational macroscopic changes in echoanatomy demonstrating reduced duodenal wall thickness (DUOTHICK = 0.489 cm) (Figure 5B, double white arrowheads), reduced wall echogenicity, recovery of the normal arrangement of the tri-layer wall structure, the appearance of duodenal folds of Kerckring (Figure 5B, white arrow), and no HFF in the duodenal lumen. The sixth-month follow-up test (HbA1C = 6.3%) achieved the primary endpoint (HbA1C < 6.5%). Treatment of diabetic patients with IPIs using metronidazole and albendazole, in addition to antidiabetic drugs, improved the control of FBG in all patients.

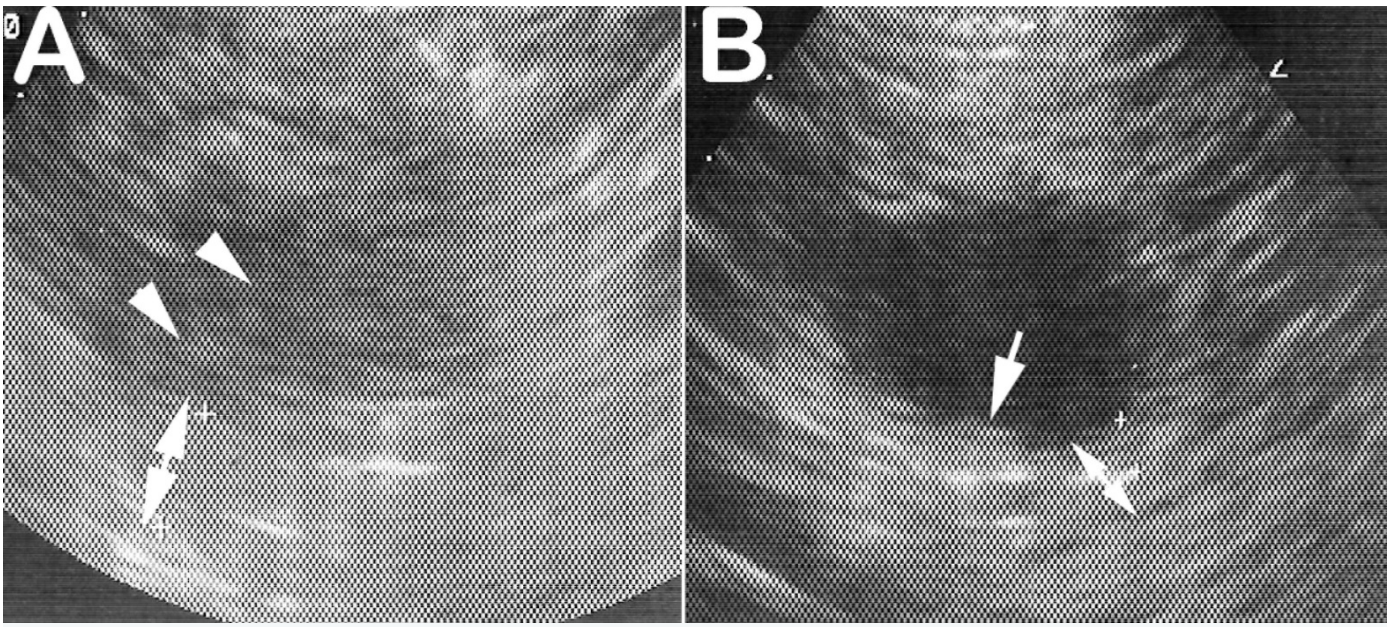

Figure 5. (**A**, **B**): Sonographic appearance of the duodenum in a diabetic patient in pretreatment (**A**) showing increased echogenicity and wall thickness (double white arrowheads) with intraluminal HFF (white arrowheads); (**B**) in post-treatment, shows duodenal folds of Kerckring (white arrow), the wall thickness (double white arrowheads) and echogenicity are reduced and there is no HFF.

4. Discussion

Our findings suggest that patients were exposed to contaminated food and water, which led to infection with IPIs. In the present study, we did not analyze the microbiome. However, we hypothesized that IPIs cause dysbiosis of the intestinal microbiome. We further hypothesized that the resulting inflammatory processes led to the dysfunction of the cytoskeleton in the intestinal wall. The dysfunction of the cytoskeleton creates a neuromuscular imbalance, which in turn leads to an imbalance in the autonomic nervous system. This imbalance has local effects on intestinal motility and overall effects on diastolic blood pressure. The increase in sympathetic activity may be implicated in both initiating and sustaining the elevation in diastolic blood pressure. The autonomic innervation of the small and large intestines is provided by extrinsic sympathetic and parasympathetic fibers. The innervation of the colon depends on its embryological origin [34][35]. The ascending colon and the proximal two-thirds of the transverse colon, which originate from the midgut, receive their sympathetic, parasympathetic, and sensory innervation through nerves from the superior mesenteric plexus. On the other hand, the distal one-third of the transverse colon, descending colon, and sigmoid colon receive their sympathetic, parasympathetic, and sensory supplies through nerves from the inferior mesenteric plexus. The parasympathetic innervation is derived from the pelvic splanchnic nerves, while the sympathetic innervation is received through the lumbar splanchnic nerves [34][35].

The results demonstrate changes in the macroscopic echoanatomy of the intestinal wall, depicting the rearrangement of the cytoskeleton and its transformation during the post-treatment period. The latter suggests that the effects of IPIs on cytoskeletal dysfunction disrupt the electrogenic mechanism in the well-organized colonic intestinal epithelium. The cumulative effects of IPI-induced dysbiosis and rearrangement of the colonic wall cytoskeleton could lead to several

outcomes. These include the inactivation of electrogenic sodium transport [40], immune system response [41], increased production of short-chain fatty acids (SCFAs) by intestinal bacteria [42], elevated levels of lipopolysaccharides (LPS) or endotoxin from the outer cell wall of gram-negative bacteria [43], and elevated blood sugar levels due to poor regulation of glucose transporters [29][30]. The sequence of events can be summarized by the steps illustrated in Figure 6. The cumulative effects of IPIs on the intestinal wall result in a "leaky gut." Hence, we propose a theory of the "Leaky Intestine" or "Leaky Gut" caused by the impact of IPIs and the intestinal microbiome. The main pathogenetic steps are outlined in the schematic diagram (Figure 6).

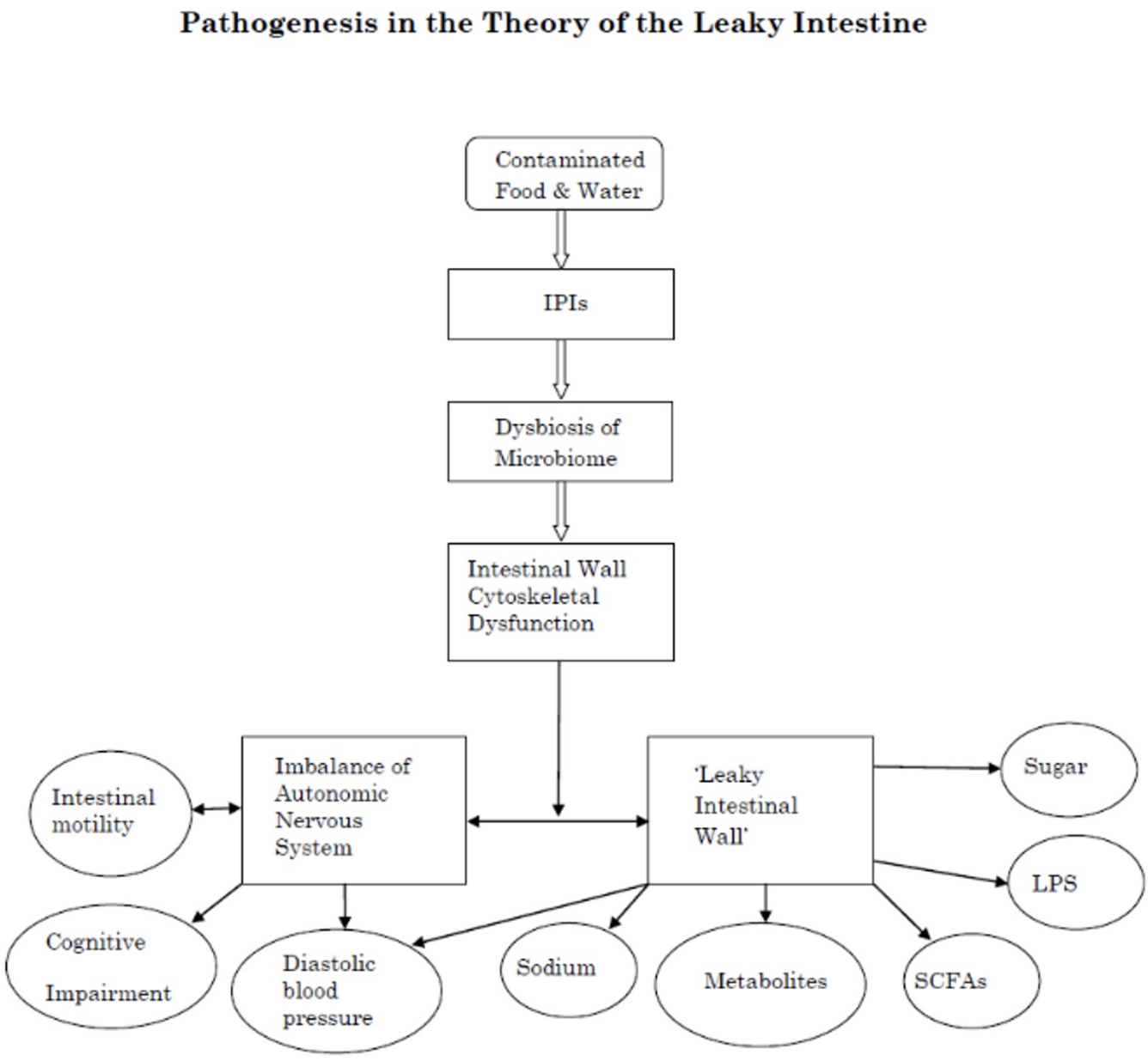

Figure 6. Illustrates the pathogenetic steps involved in the development of a 'leaky intestine'.

The significant changes in wall echogenicity observed from pretreatment to post-treatment indicate an increase in blood flow, which promotes tissue regeneration of the intestinal wall cytoskeleton. These tissue regenerations resulted in the

“sealing of the intestinal wall leak.” This may indicate a potential role for innovative stem cell therapy in the “sealing of the intestinal wall.” Moreover, investigators have suggested the use of mesenchymal stem cell (MSC) therapy for managing inflammatory bowel disease (IBD). This therapy primarily aims to reduce inflammation, regulate immune disorders, and promote the repair of mucosal tissue [37][44][45]. While the use of MSCs after severe IPIs is yet unexplored, conducting an exploratory study could be beneficial.

The role of gender may offer insights into potential new treatment strategies for sealing the leaky intestine. The thickness of the descending colon wall did not differ between men and women under 50 years of age. However, in individuals over 50 years, the thickness of the intestinal wall was significantly greater in men compared to postmenopausal women (>50 years). This indicates that postmenopausal women with low levels of circulating estrogen/progesterone experienced a decrease in intestinal wall thickness and cytoskeletal dysfunction, leading to “sealing the leak” [46]. Conversely, no such difference was observed in men, suggesting that testosterone levels did not exert such effects. Estrogen is known to enhance the immune system, while testosterone suppresses it [41]. One plausible explanation is that in premenopausal women, estrogen’s immune-enhancing effect upregulates the immune response within the brush-border regions of the intestines. This leads to the deposition of immune complexes, resulting in the thickening of the intestinal wall. In the postmenopausal phase, the reduced estrogen effects lead to thinner intestinal wall thickness. Additionally, some suggest that the intestinal microbiome regulates estrogens by secreting β-glucuronidase, an enzyme that deconjugates estrogens into their active forms. Intestinal parasitic infections (IPIs) disrupt this process due to the dysbiosis of the intestinal microbiome, characterized by decreased microbial diversity. The decrease in deconjugation results in reduced circulating estrogen. Changes in circulating estrogens may contribute to conditions associated with obesity, metabolic syndrome, cancer, endometrial hyperplasia, endometriosis, polycystic ovary syndrome, fertility, cardiovascular disease (CVD), and cognitive function [46].

Modulation of the microbiome composition is presumed to subsequently impact the metabolic profile, and vice versa. Such modulation has been shown to alleviate many disease states regulated by estrogen [46]. These considerations suggest that estrogen antagonists, such as tamoxifen, could be potential candidates for “sealing the leak” of the intestine [47]. Furthermore, researchers have demonstrated the antimicrobial activity of tamoxifen metabolites against multidrug-resistant (MDR) strains of *Acinetobacter baumannii* and *Escherichia coli*. Tamoxifen may present a potential alternative for treating infections caused by these pathogens [47][48].

The absorption of water and salts through a ‘leaky intestine’ would be abnormal. Water diffuses in response to an osmotic gradient established by electrolyte absorption. Sodium is actively absorbed in the intestine through sodium channels [40]. As the intestinal wall thickens due to cytoskeletal rearrangement, sodium channels become inactivated, disrupting the osmotic gradient on both sides of the intestinal brush border membrane (BBM). BBM permeability plays a pivotal role in regulating blood sodium levels. These levels can vary from hyponatremia to hypernatremia during the course of an IPI-related illness in the same patient.

Recently, we proposed a mechanism linking IPIs and T2DM [29]. Repeated infections in childhood and adulthood resulted in the rearrangement of the intestinal cytoskeleton, leading to the malfunction of the glucose transporter system [49][50]. In

the well-organized small intestinal epithelium, the main mechanism of dietary glucose transport from the intestinal lumen into enterocytes involves SGLT1 and GLUT2 [49][50][51][52][53]. Our study demonstrated that IPIs effects induce changes in the macroscopic echoanatomy of the intestinal wall, indicative of cytoskeletal rearrangement [29]. Therefore, we posit that the cytoskeleton rearrangement compromises the membrane potential of IECs, affecting the regulation of SGLT1 and GLUT2 activity. This disruption in regulation could result in the nonselective transport of complex carbohydrates, hydrolyzed into monosaccharides, such as glucose or galactose, across the intestinal mucosa. The cumulative effects of IPI-induced cytoskeletal rearrangement could lead to increased FBG levels. Alongside factors such as age, obesity, and genetic predisposition, this could contribute to T2DM development. In our current study, we observed that patients with parasites displayed a higher BMI (mean = 28.98 ± 7.43) in comparison to controls (mean = 24.68 ± 7.2), particularly among men. This finding implies a potential link between obesity and intestinal parasitic infections (IPIs). Further studies are warranted to investigate potential antidiabetic drugs, such as SGLT1 inhibitors, as candidates for sealing the ‘intestinal leak’. The current study observed only a small number of diabetic patients, necessitating further research.

It is plausible that natural compounds could alleviate the effects of IPI-induced rearrangement of the intestinal wall cytoskeleton through direct interactions with the intestinal microbiome. Several natural compounds with potential antidiabetic properties include fukugetin, palmatine, berberine, honokiol, amorfrutins, trigonelline, gymnemic acids, gurmarin, and phlorizin [54]. Additionally, specific natural extracts, such as *Aframomum melegueta*, might exert direct antibacterial effects [55] on IPI-induced dysbiosis.

We observed a significant inverse correlation between the thickening of the intestinal wall in the descending colon and the blood sodium level. In simpler terms, as the intestinal wall thickened, the electrogenic mechanisms controlling blood sodium levels malfunctioned, resulting in reduced Na^+ and water absorption. Similarly, prior research has established a notable inverse correlation between the thickness of the intestinal wall in the descending colon and diastolic blood pressure. The decrease in blood sodium levels resulting from shifts in osmolar gradients across the brush border membrane (BBM) may lead to reduced diastolic blood pressure, while systolic blood pressure remains unaffected. Moreover, previous studies have indicated that urinary sodium excretion is linked to diastolic blood pressure, but not systolic blood pressure in hypertensive patients. This relationship accounts for 17% of the variability in diastolic blood pressure [56].

In conclusion, we have demonstrated the effects of IPIs on the intestinal microbiome and the development of a “leaky gut”. The IPIs lead to dysbiosis of the intestinal microbiome, which in turn causes dysfunction of the cytoskeleton of the intestinal wall. This disruption creates a neuromuscular imbalance, which in turn triggers an autonomic nervous system imbalance. This disruption has both localized effects on intestinal peristalsis and general effects on diastolic blood pressure. The cumulative impact of IPI-induced changes in the colonic wall’s cytoskeleton could elevate sodium levels, SCFAs [41], LPS-sugar, and immune system activation [57][58]. This set of conditions manifests as a complex syndrome, aptly described as the ‘leaky gut syndrome’. The primary pathogenetic steps are outlined in the provided schematic diagram. Notably, the significant changes in wall echogenicity observed from pretreatment to post-treatment effects indicate an increase in blood flow, which contributes to tissue regeneration in the intestinal wall. We suggest the exploration of innovative stem cell therapy for “sealing the leak” in the intestinal wall [37][44]. Furthermore, the role of

gender may offer insights into potential novel treatment drugs for sealing the leaky intestine [46][47]. The central mechanism underpinning “leaky gut syndrome” is the disruption of intestinal permeability [59][60].

While the findings of our present pilot study offer valuable insights, it is essential to acknowledge the limited sample size. Therefore, further research involving larger and more diverse cohorts is imperative. These studies should also encompass microbiome analysis employing rigorous statistical techniques for assessing primary endpoints.

Statements and Declarations

Author Contributions: Conceptualization, P.C.N.; Methodology, P.C.N., J.E.O., C.C.D., N.E.U., C.O.M., C.C.O., C.O., C.O.U., L.O.U., M.A., F.N.O. and L.C.M.; Formal analysis, P.C.N.; Investigation, P.C.N., A.A., J.E.O., C.C.D., N.E.U., C.O.M., C.C.O., C.O., C.O.U., L.O.U., M.A., F.N.O. and L.C.M.; Data curation, P.C.N. All authors have read and agreed to the published version of the manuscript.

Funding: This research received no funding.

Institutional Review Board Statement: The study was conducted in accordance with the Declaration of Helsinki, and approved by the Institutional Review Board of Chidicon Medical Center, International Institutes of Advanced Research and Training, (protocol code IRB2020/03/H003; approved March 15th 2020) for studies involving humans.

Informed Consent Statement: Informed consent was obtained from all subjects involved in the study.

Data Availability Statement: No data links are available.

Conflicts of interest: There are no conflict of interest.

References

1. ^*Yoseph, A.; Beyene, H. The high prevalence of intestinal parasitic infections is associated with stunting among children aged 6–59 months in Boricha Woreda, Southern Ethiopia: A cross-sectional study. BMC Public Health 2020, 20, 1270. https://doi.org/10.1186/s12889-020-09377-y.*
2. ^*Teimouri, A.; Alimi, R.; Farsi, S.; Mikaeili, F. Intestinal parasitic infections among patients referred to hospitals affiliated to Shiraz University of Medical Sciences, southern Iran: A retrospective study in pre- and post-COVID-19 pandemic. Environ. Sci. Pollut. Res. Int. 2022, 29, 36911–36919. https://doi.org/10.1007/s11356-021-18192-w.*
3. ^*Njenga, D.; Mbugua, A.K.; Okoyo, C.; Njenga, S.M. Intestinal parasite infections and associated risk factors among pre-school aged children in Kibera Informal Settlement, Nairobi, Kenya. East Afr. Health Res. J. 2022, 6, 86–97. https://doi.org/10.24248/eahrj.v6i1.683.*
4. ^*Melese, M.; Birhan, T.A.; Simegn, W.; Adugna, D.G.; Diress, M.; Getawa, S.; Azanaw, J. Prevalence of Diarrhea, Intestinal Parasites, and Associated Factors Among Under-Five Children in Dabat District, Northwest Ethiopia:*

Multicenter Cross-sectional Study. Environ. Health Insights 2023, 17, 11786302231174744. https://doi.org/10.1177/11786302231174744.

5. ^*Ambachew, S.; Assefa, M.; Tegegne, Y.; Zeleke, A.J. The Prevalence of Intestinal Parasites and Their Associated Factors among Diabetes Mellitus Patients at the University of Gondar Referral Hospital, Northwest Ethiopia. J. Parasitol. Res. 2020, 2020, 8855965. https://doi.org/10.1155/2020/8855965.*
6. ^*Zibaei, M.; Bahadory, S.; Saadati, H.; Pourrostami, K.; Firoozeh, F.; Foroutan, M. Intestinal parasites and diabetes: A systematic review and meta-analysis. New Microbes New Infect. 2022, 51, 101065.*
7. ^*Ray, A.; Bonorden, M.J.L.; Pandit, R.; Nkhata, K.J.; Bishayee, A. Infections and immunity: Associations with obesity and related metabolic disorders. J. Pathol. Transl. Med. 2023, 57, 28–42.*
8. a, b, c*Von Huth, S.; Thingholm, L.B.; Kofoed, P.-E.; Bang, C.; Rühlemann, M.C.; Franke, A.; Holmskov, U. Intestinal protozoan infections shape fecal bacterial microbiota in children from Guinea-Bissau. PLoS Negl. Trop. Dis. 2021, 15, e0009232. https://doi.org/10.1371/journal.pntd.0009232.*
9. ^*Eyayu, T.; Kiros, T.; Workineh, L.; Sema, M.; Damtie, S.; Hailemichael, W.; Dejen, E.; Tiruneh, T. Prevalence of intestinal parasitic infections and associated factors among patients attending at Sanja Primary Hospital, Northwest Ethiopia: An institutional-based cross-sectional study. PLoS ONE 2021, 16, 0247075. https://doi.org/10.1371/journal.pone.0247075.*
10. a, b*Funso-Aina, O.I.; Chineke, H.N.; Adogu, P.O. A Review of Prevalence and Pattern of Intestinal Parasites in Nigeria (2006–2015). Eur. J. Med. Health Sci. 2020, 2, 1–6. https://doi.org/10.24018/ejmed.2020.2.1.139.*
11. ^*Ogonaka, I.A.; Nwoke, B.E.B.; Ukaga, G.N. Prevalence of Soil Transmitted Helminthes among Primary School Pupils in Owerri West Local Government Area in Imo State, Nigeria. Parasitol. Public Health Soc. Niger. 2011, 27, 92.*
12. ^*Opara, K.N.; Nwoke, E.A.; Abanobi, C.O.; Onwuliri, C.O.E.; Iwuala, C.; Amadi, A.N. Intestinal parasites among children in day-care centres in Owerri metropolis Nigeria. Niger. J. Parasitol. 2010, 31, 45–49.*
13. a, b*Ahmed, S.; Spence, J.D. Sex differences in the intestinal microbiome: Interactions with risk factors for atherosclerosis and cardiovascular disease. Biol. Sex Differ. 2021, 12, 35. https://doi.org/10.1186/s13293-021-00378-z.*
14. ^*Fransen, F.; van Beek, A.A.; Borghuis, T.; Meijer, B.; Hugenholtz, F.; van der Gaast-de Jongh, C.; Savelkoul, H.F.; de Jonge, M.I.; Faas, M.M.; Boekschoten, M.V.; et al. The Impact of Gut Microbiota on Gender-Specific Differences in Immunity. Front. Immunol. 2017, 8, 754. https://doi.org/10.3389/fimmu.2017.00754.*
15. ^*Dan, X.; Mushi, Z.; Baili, W.; Han, L.; Enqi, W.; Huanhu, Z.; Shuchun, L. Differential analysis of hypertension-associated intestinal microbiota. Int. J. Med. Sci. 2019, 16, 872–881. https://doi.org/10.7150/ijms.29322.*
16. ^*De la Cuesta-Zuluaga, J.; Mueller, N.T.; Álvarez-Quintero, R.; Velásquez-Mejía, E.P.; Sierra, J.A.; Corrales-Agudelo, V.; Carmona, J.A.; Abad, J.M.; Escobar, J.S. Higher fecal short-chain fatty acid levels are associated with gut microbiome dysbiosis, obesity, hypertension and cardiometabolic disease risk factors. Nutrients 2018, 11, 51. https://doi.org/10.3390/nu11010051.*
17. ^*Li, J.; Zhao, F.; Wang, Y.; Chen, J.; Tao, J.; Tian, G.; Wu, S.; Liu, W.; Cui, Q.; Geng, B.; et al. Gut microbiota dysbiosis contributes to the development of hypertension. Microbiome 2017, 5, 14. https://doi.org/10.1186/s40168-016-0222-x.*

18. ^Sun, S.; Lulla, A.; Sioda, M.; Winglee, K.; Wu, M.C.; Jacobs, D.R., Jr.; Shikany, J.M.; Lloyd-Jones, D.M.; Launer, L.J.; Fodor, A.A.; et al. Gut microbiota composition and blood pressure. Hypertension 2019, 73, 998–1006. https://doi.org/10.1161/HYPERTENSIONAHA.118.12109.
19. ^Verhaar, B.J.H.; Collard, D.; Prodan, A.; Levels, J.H.M.; Zwinderman, A.H.; Bäckhed, F.; Vogt, L.; Peters, M.J.L.; Muller, M.; Nieuwdorp, M.; et al. Associations between gut microbiota, faecal short-chain fatty acids, and blood pressure across ethnic groups: The HELIUS study. Eur. Heart J. 2020, 41, 4259–4267. https://doi.org/10.1093/eurheartj/ehaa704.
20. ^Yan, Q.; Gu, Y.; Li, X.; Yang, W.; Jia, L.; Chen, C.; Han, X.; Huang, Y.; Zhao, L.; Li, P.; et al. Alterations of the gut microbiome in hypertension. Front. Cell Infect. Microbiol. 2017, 7, 381. https://doi.org/10.3389/fcimb.2017.00381.
21. ^Yang, T.; Santisteban, M.M.; Rodriguez, V.; Li, E.; Ahmari, N.; Carvajal, J.M.; Zadeh, M.; Gong, M.; Qi, Y.; Zubcevic, J.; et al. Gut dysbiosis is linked to hypertension. Hypertension 2015, 65, 1331–1340. https://doi.org/10.1161/HYPERTENSIONAHA.115.05315.
22. ^Kim, S.; Goel, R.; Kumar, A.; Qi, Y.; Lobaton, G.; Hosaka, K.; Mohammed, M.; Handberg, E.M.; Richards, E.M.; Pepine, C.J.; et al. Imbalance of gut microbiome and intestinal epithelial barrier dysfunction in patients with high blood pressure. Clin. Sci. 2018, 132, 701–718. https://doi.org/10.1042/CS20180087.
23. ^Huart, J.; Leenders, J.; Taminiau, B.; Descy, J.; Saint-Remy, A.; Daube, G.; Krzesinski, J.-M.; Melin, P.; de Tullio, P.; Jouret, F. Gut microbiota and fecal levels of short-chain fatty acids differ upon 24-hour blood pressure levels in men. Hypertension 2019, 74, 1005–1013. https://doi.org/10.1161/HYPERTENSIONAHA.118.12588.
24. ^Jackson, M.A.; Verdi, S.; Maxan, M.E.; Shin, C.M.; Zierer, J.; Bowyer, R.C.E.; Martin, T.; Williams, F.M.K.; Menni, C.; Bell, J.T.; et al. Gut microbiota associations with common diseases and prescription medications in a population-based cohort. Nat. Commun. 2018, 9, 2655. https://doi.org/10.1038/s41467-018-05184-7.
25. ^Adeloye, D.; Owolabi, E.O.; Ojji, D.B.; Auta, A.; Dewan, M.T.; Olanrewaju, T.O.; Ogah, O.S.; Omoyele, C.; Ezeigwe, N.; Mpazanje, R.G.; et al. Prevalence, awareness, treatment, and control of hypertension in Nigeria in 1995 and 2020: A systematic analysis of current evidence. J. Clin. Hypertens. 2021, 23, 963–977.
26. ^Odili, A.; Chori, B.; Danladi, B.; Nwakile, P.; Okoye, I.; Abdullah, U.; Nwegbu, M.N.; Zawaya, K.; Essien, I.; Sada, K.; et al. Prevalence, Awareness, Treatment and Control of Hypertension in Nigeria: Data from a Nationwide Survey 2017. Glob. Heart 2020, 15, 47. https://doi.org/10.5334/gh.848.
27. ^Mohanty, P.; Patnaik, L.; Nayak, G.; Dutta, A. Gender difference in prevalence of hypertension among Indians across various age-groups: A report from multiple nationally representative samples. BMC Public Health 2022, 22, 1524. https://doi.org/10.1186/s12889-022-13949-5.
28. ^Akinlua, J.T.; Meakin, R.; Umar, A.M.; Freemantle, N. Current Prevalence Pattern of Hypertension in Nigeria: A Systematic Review. PLoS ONE 2015, 10, e0140021. https://doi.org/10.1371/journal.pone.0140021.
29. a, b, c, d, e, f, g, h, i, j, k, l, m, n, o, p, qNjemanze, P.C.; Darlington, C.C.; Onuchukwu, J.E.; Ukeje, N.E.; Amadi, A.; Mgbenu, C.U.; Mezu, C.O.; Anaele, J.C.; Okoro, M.O.; Nneke, E.; et al. Intestinal parasitic infection-induced intestinal wall cytoskeleton dysfunction in diabetes mellitus. Niger. J. Gen. Pract. 2022, 20, 29–35.
30. a, b, cSun, D.; Xiang, H.; Yan, J.; He, L. Intestinal microbiota: A promising therapeutic target for hypertension. Front. Cardiovasc. Med. 2022, 9, 970036. https://doi.org/10.3389/fcvm.2022.970036.

31. [a, b, c, d, e, f, g, h, i, j, k, l, m, n, o, p, q]*Njemanze, P.C.; Njemanze, J.; Skelton, A.; Akudo, A.; Akagha, O.; Chukwu, A.A.; Peters, C.; Maduka, O. High-frequency ultrasound imaging of the duodenum and colon in patients with symptomatic giardiasis in comparison to amebiasis and healthy subjects. J. Gastroenterol. Hepatol. 2008, 23, e34–e42.*
32. [a, b, c, d]*Njemanze, P.C.; Njemanze, J.T.; Ofoegbu, C.C.; Darlington, C.C.; Nneke, E.; Onweni, J.A.; Ejiogu, U.V.; Mgbenu, C.U.; Ukeje, N.E.; Amadi, A.C.; et al. High-frequency ultrasound imaging of the intestine in normal subjects and patients with intestinal parasites. In Essentials of Abdominal Ultrasound; Ali Abdo Gamie, S., Mahmoud Foda, E., Eds.; IntechOpen: London, UK, 2019; pp. 91–105.*
33. [a, b, c, d, e, f, g, h, i, j, k, l, m]*Njemanze, P.C.; Njemanze, J.T.; Ofoegbu, C.C.; Nneke, E.; Onweni, I.A.; Ejiogu, U.V.; Mgbenu, C.U.; Ukeje, N.E.; Amadi, A.C.; Amaefule, D.C. Technical notes on high-frequency ultrasound duodenography and colonography imaging of giardial lesions. Niger. J. Gen. Pract. 2021, 19, 54–60.*
34. [a, b, c]*Zubcevic, J.; Richards, E.M.; Yang, T.; Kim, S.; Sumners, C.; Pepine, C.J.; Raizada, M.K. Impaired Autonomic Nervous Sys-tem-Microbiome Circuit in Hypertension. Circ. Res. 2019, 125, 104–116. https://doi.org/10.1161/CIRCRESAHA.119.313965.*
35. [a, b, c]*Straub, R.; Wiest, R.; Strauch, U.; Harle, P.; Schölmerich, J. The role of the sympathetic nervous system in intestinal inflam-mation. Gut 2006, 55, 1640–1649.*
36. [^]*Jeong, J.; Kim, K.; Lim, D.; Kim, K.; Kim, H.; Lee, S.; Song, H.; Moon, B.-G.; Choy, H.E.; Park, S.C. Microvasculature remodel-ing in the mouse lower gut during inflammaging. Sci. Rep. 2017, 7, 39848. https://doi.org/10.1038/srep39848.*
37. [a, b, c]*Liu, A.; Wang, X.; Liang, X.; Wang, W.; Li, C.; Qian, J.; Zhang, X. Human umbilical cord mesenchymal stem cells regulate immunoglobulin a secretion and remodel the diversification of intestinal microbiota to improve colitis. Front. Cell Infect. Mi-crobiol. 2022, 12, 960208. https://doi.org/10.3389/fcimb.2022.960208.*
38. [a, b]*American Diabetes Association. 2. Classification and diagnosis of diabetes: Standards of medical care in diabetes—2020. Dia-betes Care 2020, 43, S14–S31.*
39. [^]*National High Blood Pressure Education Program. The Seventh Report of the Joint National Committee on Prevention, Detection, Evaluation, and Treatment of High Blood Pressure; Classification of Blood Pressure; National Heart, Lung, and Blood Institute: Bethesda, MD, USA, 2004. Available online: https://www.ncbi.nlm.nih.gov/books/NBK9633/ (accessed on 14 February 2021).*
40. [a, b, c]*Azzouz, L.L.; Sharma, S. StatPearls; StatPearls Publishing: St. Petersburg, FL, USA, 2023. Available online: https://www.ncbi.nlm.nih.gov/books/NBK507857/ (accessed on 8 June 2023).*
41. [a, b, c]*Taneja, V. Sex hormones determine immune response. Front. Immunol. 2018, 9, 1931.*
42. [^]*Cong, J.; Zhou, P.; Zhang, R. Intestinal Microbiota-Derived Short Chain Fatty Acids in Host Health and Disease. Nutrients 2022, 14, 1977. https://doi.org/10.3390/nu14091977.*
43. [^]*An, L.; Wirth, U.; Koch, D.; Schirren, M.; Drefs, M.; Koliogiannis, D.; Nieß, H.; Andrassy, J.; Guba, M.; Bazhin, A.V.; et al. The Role of Gut-Derived Lipopolysaccharides and the Intestinal Barrier in Fatty Liver Diseases. J. Gastrointest. Surg. 2022, 26, 671–683. https://doi.org/10.1007/s11605-021-05188-7.*
44. [a, b]*Koppula, S.; Kumar, H. More than a pore: The therapeutic potential of stem cells for neurological disorders. Cell Tissue Res. 2019, 375, 11–24. https://doi.org/10.1007/s00441-018-2924-x.*
45. [^]*Kasemeier-Kulesa J. C., Morrison, J. A., Lefcort, F., KulesaP. M.. TrkB/BDNF signalling patterns the sympathetic*

nervous system. Nat. Commun. 2015, 6, 8281. https://doi.org/10.1038/ncomms9281.

46. [a, b, c, d]*Baker, J.M.; Al-Nakkash, L.; Herbst-Kralovetz, M.M. Estrogen-gut microbiome axis: Physiological and clinical implications. Maturitas 2017, 103, 45–53. https://doi.org/10.1016/j.maturitas.2017.06.025.*
47. [a, b, c]*Miró-Canturri, A.; Ayerbe-Algaba, R.; Vila-Domínguez, A.; Jiménez-Mejías, M.E.; Pachón, J.; Smani, Y. Repurposing of the Tamoxifen Metabolites to Combat Infections by Multidrug-Resistant Gram-Negative Bacilli. Antibiotics 2021, 10, 336. https://doi.org/10.3390/antibiotics10030336.*
48. [^]*Yang, X.; Guo, Y.; He, J.; Zhang, F.; Sun, X.; Yang, S.; Dong, H. Estrogen and estrogen receptors in the modulation of gastrointestinal epithelial secretion. Oncotarget 2017, 8, 97683–97692. https://doi.org/10.18632/oncotarget.18313.*
49. [a, b]*Gribble, F.M.; Williams, L.; Simpson, A.K.; Reimann, F. A novel glucose-sensing mechanism contributing to glucagon-like peptide-1 secretion from the GLUTag cell line. Diabetes 2003, 52, 1147–1154.*
50. [a, b]*Röder, P.V.; Geillinger, K.E.; Zietek, T.S.; Thorens, B.; Koepsell, H.; Daniel, H. The role of SGLT1 and GLUT2 in intestinal glucose transport and sensing. PLoS ONE 2014, 9, e89977.*
51. [^]*Boudry, G.; Cheeseman, C.I.; Perdue, M.H. Psychological stress impairs Na+-dependent glucose absorption and increases GLUT2 expression in the rat jejunal brush-border membrane. Am. J. Physiol. Regul. Integr. Comp. Physiol. 2007, 292, R862–R867.*
52. [^]*Chaudhry, R.M.; Scow, J.S.; Madhavan, S.; Duenes, J.A.; Sarr, M.G. Acute enterocyte adaptation to luminal glucose: A post-translational mechanism for rapid apical recruitment of the transporter GLUT2. J. Gastrointest. Surg. 2012, 16, 312–319.*
53. [^]*Koepsell, H. Glucose transporters in the small intestine in health and disease. Pflugers Arch. 2020, 472, 1207–1248. https://doi.org/10.1007/s00424-020-02439-5.*
54. [^]*Ríos, J.L.; Francini, F.; Schinella, G.R. Natural Products for the Treatment of Type 2 Diabetes Mellitus. Planta Med. 2015, 81, 975–994. https://doi.org/10.1055/s-0035-1546131.*
55. [^]*Olajuyigbe, O.O.; Adedayo, O.; Coopoosamy, R.M. Antibacterial Activity of Defatted and Nondefatted Methanolic Extracts of Aframomum melegueta K. Schum. against Multidrug-Resistant Bacteria of Clinical Importance. Scientif. World J. 2020, 2020, 4808432. https://doi.org/10.1155/2020/4808432.*
56. [^]*Cheung, B.M.; Ho, S.P.; Cheung, A.H.; Lau, C.P. Diastolic blood pressure is related to urinary sodium excretion in hypertensive Chinese patients. QJM 2000, 93, 163–168. https://doi.org/10.1093/qjmed/93.3.163. PMID: 10751235.*
57. [^]*Fasano, A. Leaky gut and autoimmune diseases. Clin. Rev. Allergy Immunol. 2012, 42, 71–78. https://doi.org/10.1007/s12016-011-8291-x.*
58. [^]*Mu, Q.; Kirby, J.; Reilly, C.M.; Luo, X.M. Leaky gut as a danger signal for autoimmune diseases. Front. Immunol. 2017, 8, 598. https://doi.org/10.3389/fimmu.2017.00598.*
59. [^]*Bischoff, S.C.; Barbara, G.; Buurman, W.; Ockhuizen, T.; Schulzke, J.D.; Serino, M.; Tilg, H.; Watson, A.; Wells, J.M. Intestinal permeability—A new target for disease prevention and therapy. BMC Gastroenterol. 2014, 14, 189. https://doi.org/10.1186/s12876-014-0189-7.*
60. [^]*Hollander, D. Intestinal permeability, leaky gut, and intestinal disorders. Curr. Gastroenterol. Rep. 1999, 1, 410–416. https://doi.org/10.1007/s11894-999-0054-6.*